Strain-modulated Mott transition in EuNiO$_3$ ultrathin films

D. Meyers,[1,*] S. Middey,[1] M. Kareev,[1] M. van Veenendaal,[2] E. J. Moon,[1] B. A. Gray,[1] Jian Liu,[3,4]
J. W. Freeland,[5] and J. Chakhalian[1]

[1]*Department of Physics, University of Arkansas, Fayetteville, Arkansas 72701, USA*
[2]*Department of Physics, Northern Illinois University, De Kalb, Illinois 60115, USA*
[3]*Department of Physics, University of California, Berkeley, California 94720, USA*
[4]*Materials Science Division, Lawrence Berkeley National Laboratory, Berkeley, California 94720, USA*
[5]*Advanced Photon Source, Argonne National Laboratory, Argonne, Illinois 60439, USA*

A series of ultrathin epitaxial films of EuNiO$_3$ (ENO) were grown on a set of substrates traversing from compressive (-2.4%) to tensile ($+2.5\%$) lattice mismatch. On moving from tensile to compressive strain, transport measurements demonstrate a successively suppressed Mott insulating behavior eventually resulting in a complete suppression of the insulating state at high compressive strain. Corroborating these findings, resonant soft x-ray absorption spectroscopy at the Ni $L_{3,2}$ edge reveals the presence of a strong multiplet splitting in the tensile strained samples that progressively weakens with increasing compressive strain. Combined with cluster calculations, the results show how cumulatively enhanced covalency (i.e., bandwidth) between Ni d and O p orbital derived states leads to the emergent metallic ground state not attainable in the bulk ENO.

I. INTRODUCTION

Complex transition-metal oxides with correlated carriers have been at the forefront of condensed matter research towards the understanding of fundamental physics underlying several remarkable physical phenomena, including high-temperature superconductivity, colossal magnetoresistance, multiferroicity, and the thermally induced metal-insulator transition (MIT).[1–6] In particular, the temperature-driven MIT in correlated oxides has garnered a strong investigation effort over the last several decades. Understanding of the MIT and its control by external stimuli such as pressure, magnetic field, light, confinement, or chemical doping is not only interesting from the fundamental physics point of view,[7–10] but also demonstrates great opportunities for future electronic devices.[11] On the way to those goals, recent advances in material synthesis by using strain engineering have opened a new dimension in controlling the materials properties. Additionally, the epitaxial relation has been used to stabilize new structural and electronic phases in the form of ultra thin films of coherently strained materials.[12] In such epitaxially stabilized structures, the effect of the lattice modulation on the materials properties can be quite dramatic[13–26] and is of particular current interest as applications continue to accelerate towards ultrathin films and heterostructures.

The rare-earth (RE) nickelates RNiO$_3$ ($R = $ Pr, Nd, Eu, . . .) in their bulk form, with Ni having formal $+3$ oxidation state ($t_{2g}^6 e_g^1$), all, except for $R = $ La, display a metal-insulator transition, while the nature of the transition and its temperature (T_{MIT}) depend strongly on the choice of the rare-earth cation as shown in Fig. 1.[27–29] Specifically, the most distorted members with $R = $ Lu, Y, Eu, and Sm, etc. first exhibit a second-order MIT at higher temperature accompanied by the development of a possible charge ordered state,[30–34] while the magnetic moments remain disordered across the transition. Upon further cooling, these compounds undergo another second-order transition characterized by a E'-type antiferromagnetism. In

sharp contrast, the members with a smaller degree of structural distortion (e.g., $R = $ Nd and Pr) exhibit a first-order phase transition emerging directly from the paramagnetic metallic state into the E'-type antiferromagnetic insulating ground state, thus bypassing entirely the large paramagnetic insulating region.[28,35–37] Based on such a diverse behavior controlled by the A-site ion, several interesting theory proposals and experimental results have been put forward to control the MIT for potential applications;[38–41] however, using different R ions depending on application seems impractical, as synthesis conditions and thermal stability vary wildly and rarely yield macroscopic-size crystals of nickelates.[13,42–45] Alternatively, one can explore the obligatory strain in ultrathin films as a tool to engineer the physical properties based on a careful choice of a *single* member of the family to attempt to modulate the MI and antiferromagnetic (AFM) transitions.[13,14,46] En route to this goal, one of the key questions is what effect will strain (tensile and compressive) have upon the phase diagram given in Fig. 1 for the distorted members exhibiting the second order transitions? For example, it has been already shown in the bulk that, while isotropic external pressure suppresses the MIT, it also tends to raise the temperature for AFM transition and eventually leads to a surprising AFM in the metallic ground state;[47–49] based on this observation, one can expect highly nontrivial electronic and structural response after application of bi-axial strain.[50,51]

In this paper, we demonstrate how biaxial strain can alter basic electronic properties of ultrathin epitaxially strained EuNiO$_3$ (ENO) films grown on various substrates spanning both compressive and tensile strain. X-ray diffraction (XRD), reciprocal space mapping (RSM), electric dc transport, and resonant soft x-ray absorption spectroscopy (XAS) are applied to elucidate the microscopic effects of strain on the structural, electronic, and magnetic properties. These experiments confirm the remarkable capacity of epitaxial stabilization to modulate the physical properties of this strongly distorted
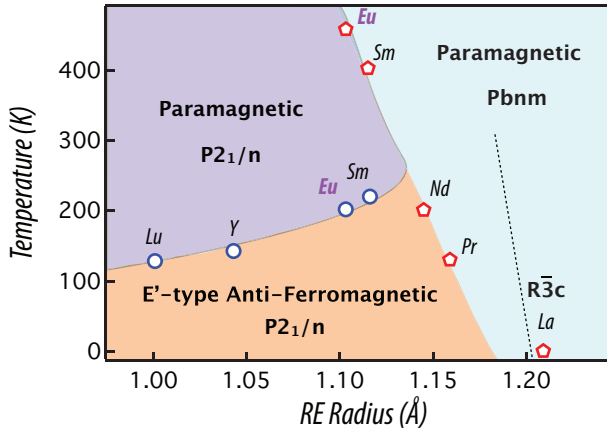
FIG. 1. (Color online) Partial phase diagram for the family of rare-earth nickelates of different *A* sites (data from Refs. 28 and 29). The dotted line represents the change from orthorhombic (*Pbnm*) to rhomohedral ($R\bar{3}C$) symmetry.

nickelate system. In addition, *ab intio* cluster calculations on a NiO_6 octahedra revealed the evolution of the charge excitation gap as a function of the strain state and the possibility of gap closing resulting in emergent metallicity, thus shedding light on the source of the marked modulation in the material's properties.

II. EXPERIMENTAL AND THEORETICAL METHODS

ENO films were grown on a variety of substrates incorporating lattice mismatch ranging from $+2.5\%$ to -2.4%, the details of which are reported elsewhere.[45] The substrates used for growth are as follows: $YAlO_3$ (YAO; -2.4% lattice mismatch), $SrLaAlO_4$ (SLAO; -1.3%), $LaAlO_3$ (LAO; -0.3%), $NdGaO_3$ (NGO; $+1.5\%$), and $LaGaO_3$ (LGO; $+2.5\%$). XRD measurements were taken around the (0 0 2) (psuedocubic notation) truncation rod of the substrate with a Panalytical X'Pert Pro materials research diffractometer (MRD) (Panalytical, Almelo), equipped with a parabolic mirror and triple-bounce/axis monochromator on the incident and diffracted beams. The same instrument was used to measure a RSM around the (-1 0 3) truncation rod. Transport properties were measured with a Quantum Design physical property measurement system (PPMS) using a four-point probe in the Van Der Pauw geometry. XAS measurements were taken at the 4-ID-C beam line of the Advanced Photon Source at Argonne National Laboratory in total electron yield (TEY) mode at the Ni $L_{2,3}$ edges at 250 K.

Theoretical calculations were performed for a NiO_6 cluster with octahedral coordination using the methods described in Refs. 52 and 53. The Hamiltonian includes the on-site Coulomb interaction between the $3d$ electrons and between the $3d$ electrons and the $2p$ core hole. The model parameters are obtained within the Hartree-Fock limit and scaled down to 80% to account for intra-atomic screening effects. The monopole parts were $F_{dd}^0 = 6$ eV and $F_{pd}^0 = 7$ eV. The spin-orbit coupling was included for the $3d$ and $2p$ electrons. The hybridization with the ligands was taken into account by including configurations up to a double ligand hole. The hybridization parameters used were $V = 2.25$ and -1.03 eV
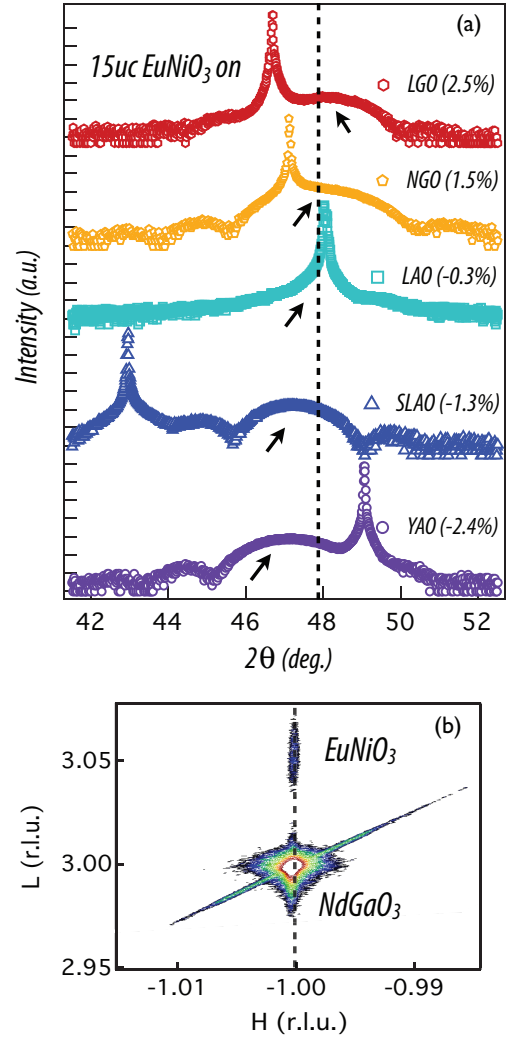

FIG. 2. (Color online) (a) XRD data for 15 uc ENO samples on various substrates. The arrows indicate the film peaks. The shifting from the bulk lattice value (indicated by the dashed line) is apparent for the compressively strained samples. Note for SLAO the (0 0 6) rod is scanned due to the tetragonal structure. The data have been artificially shifted vertically to ease inspection. (b) RSM for a 35 uc ENO film grown on NGO showing the film is coherently strained.

for the e_g and t_{2g} orbitals, respectively. The cubic crystal field of 10 Dq was set at 1.5 eV.

III. RESULTS

Figure 2(a) shows 2θ-ω scans around the (0 0 2) truncation rod for the 15 unit cell (uc) ENO films grown on different substrates. All samples show a broadened film peak (indicated by arrows), due to the reduced thickness of the films, and a sharp substrate peak which was used to align each data set. The film peaks for the highly compressive films (YAO and SLAO) show a noticeable shift from the bulk ENO lattice constant (represented by a dashed line) towards smaller 2θ, while for LAO no such shift is observed. On the other hand, films grown under tensile strain (NGO and LGO) exhibit a well resolved film peak with no measurable shift away from the bulk value. Figure 2(b) shows a RSM around
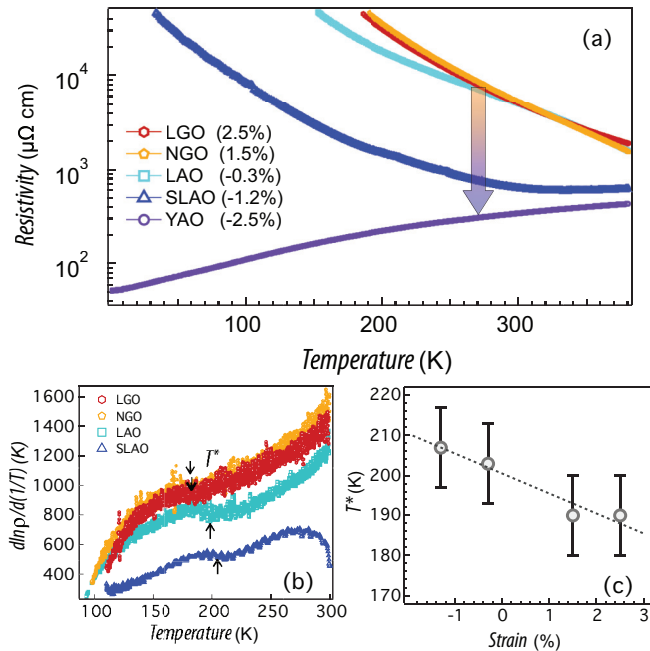
FIG. 3. (Color online) (a) Transport data for 15 uc ENO samples on various substrates. The arrow indicates the direction of increasing compressive strain. (b) $d\ln(\rho)/d(1/T)$ data for the films. Arrows indicate the location of T^*. (c) T^* for various strains.

the $(-1\,0\,3)$ Bragg peak for a 35 uc ENO on NGO film (thicker films were necessary to resolve the peak using this conventional XRD). The weak film peak shares the same value for H (reciprocal lattice units) and a larger value for L, showing the film shares the in-plane lattice constant of the substrate.

After the high structural quality was established we turned our attention to their transport properties shown in Fig 3(a). The data were recorded during both cooling and heating cycles from 380 to 2 K; since no measurable hysteresis was found only the curves measured on warming are shown. As seen, for the tensile strain the resistivity follows the expected bulklike insulating behavior below 380 K. This behavior, however, markedly changes after reversing the sign of strain. For the small compressive strain on LAO, the resistivity at lower temperatures separates from bulk behavior at ∼250 K and begins increasing at a lesser rate. For the compressively strained film on SLAO, the sample shows unexpected metallic behavior at high temperatures with a MIT occurring at 335 K. Finally, for the largest value of strain of -2.4%, the film on YAO turns metallic in the entire temperature range down to 2 K. To investigate the magnetic transition via the electrical transport, $d\ln\rho/d(\frac{1}{T})$ vs T is shown for all films besides ENO on YAO using a custom-built liquid nitrogen cryostat to reduce measurement noise which is usually amplified by the derivative analysis, in order to mimic the analysis used by Zhou *et al.*[36] Each film showed a characteristic kink indicative of an AFM transition around 200 K. Figure 3(c) shows the extracted T values for the kinks, denoted T^*.

We performed measurements at the Ni $L_{3,2}$ edges using XAS to investigate the electronic structure of our films. As seen in Fig. 4(a), all films show a strong white line at ∼855 and ∼872 eV. Additionally, a shoulder around 853 and 871 eV
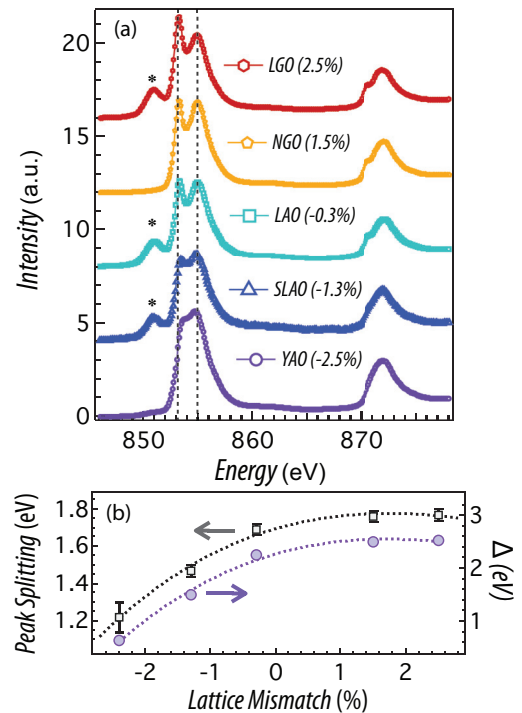

FIG. 4. (Color online) (a) XAS data for 15 uc ENO samples on various substrates showing the change in the multiplet peak with strain. The data have been artificially shifted vertically to ease inspection. (b) The experimentally obtained peak splitting along with the theoretically obtained corresponding CT energy. Note a small peak, indicated by the asterisks, around ∼ 851 eV corresponding to the La M$_4$ edge appears for the substrates containing La.

is apparent for all films, being much larger for the tensile case; this feature gradually decreases with increasing compressive strain. The size of the energy separation between the L_3 multiplet peak for each value of strain is plotted in Fig. 4(b) in the left axis. The splitting decreases from the tensile strained films, ∼1.8 eV, with increasing compressive strain to ∼1.2 eV for YAO. Figure 4(b) also shows the calculated charge transfer (CT) energy (right axis) which follows a very similar trend.

IV. DISCUSSION

The large amount of epitaxial strain built into these materials is due to the extraordinary ability of the perovskite structural units to accommodate the strain through tilts and/or rotations and through changes in lattice symmetry;[51] it is these effects that ultimately lead to the observed modulation of the physical properties. Based on this, 2θ values, corresponding to the film peaks in Fig. 2(a), were used to calculate the out-of-plane lattice constants yielding the following c-axis lattice constants: 3.86 Å (YAO), 3.84 Å (SLAO), 3.80 Å (NGO), and 3.81 Å (LGO), while for LAO strong overlap between the substrate peak and film peak due to the small strain value of -0.5% prevents a reliable c-axis lattice constant from being extracted. While for the samples with in-plane compressive strain the shift of the out-of-plane lattice constants from the bulk value of 3.80 Å is expected and consistent with tetragonal distortion of the unit cell, the samples under tensile

strain show no significant shift (e.g., 0.26% for ENO on LGO, much lower than the $+2.5\%$ biaxial in-plane strain).

To ascertain whether or not this lack of *c*-axis lattice modulation was due to strain relaxation, unlikely in ultrathin films, a RSM was taken to detect any deviation from epitaxial growth. The thicker sample (35 uc) was required in order to obtain a strong enough $(-1\,0\,3)$ film peak with the conventional source XRD. The *H* value of this film peak matches well with that of the substrate (demonstrated by the dotted line) confirming the film is fully coherent to the substrate (as was found for ENO on YAO[45]), while the center *L* value of $\sim$3.053 reciprocal lattice units (r.l.u.) gives an out-of-plane lattice constant of 3.793 Å, in excellent agreement with the rocking curve measurement (within 0.2%). This, along with the bulk-like *c*-axis lattice constant, implies the strain is compensated for by octahedral tilts and rotations, similar to that found for $LaNiO_3$ films under tensile strain.[51,54] Further work including x-ray linear dichroism (XLD) measurements and density-functional theory calculations need to be performed in order to confirm this.

Tracking the evolution of the MIT with lattice modulation revealed a very significant effect. As compressive strain is increased T_{MIT} is gradually suppressed until entirely disappearing for the case of ENO on YAO. In the case of intermediate compressive strain on SLAO, the linear *T*-dependent metallic behavior is followed by a MIT shifted to 335 K, putting it very close to room temperature. Unfortunately, the high temperature of the bulk MIT (480 K) prevents us from investigating the change in the T_{MIT} for LAO, NGO, and LGO films. With the lack of hysteresis, characteristic of first-order phase transitions, our results strongly imply that epitaxial strain does not induce a first-order transition in this material, as was seen in the bulk by application of "chemical" pressure.[37] Instead the results show that compressive strain acts to lower the transition temperatures akin to isotropic external pressure.[36,48,49] The resistivity results are also strongly reminiscent of behavior of ultrathin films of $NdNiO_3$, where it was proposed that a closing of the correlated gap is responsible for the quenching of the MIT by compressive strain.[13]

The ultrathin nature of the samples precludes direct investigation of the sample by way of conventional magnetometry. In an attempt to locate the AFM transition temperature, $d\ln\rho/d(\frac{1}{T})$ was extracted for all insulating samples; this analysis allowed Zhou *et al.* to reveal a characteristic spin ordering temperature in the bulk nickelates where spin ordering appears as a kink in the *T* dependence.[36] As seen in Fig. 3(c), all the films exhibit a broadened kink around T^*. The error bars are meant to represent the approximate width of the kink, which is similar for all samples. The magnitude of T^* is approximately 12 K lower for the tensile strained samples and is similar to the change reported for external pressure.[36] For LAO, with very small compressive strain, the value is shifted upward to 203 K. For SLAO the value of T^* is further shifted to 207 K, indicating that the Neel temperature for these films is shifted higher with higher value strain, analogous to the effect of external pressure reported by Zhou *et al.*[36] Resonant x-ray scattering measurements are needed in order to further confirm these changes in T_N and investigate any possible changes in magnetic structure, which cannot be deduced via transport.

Resonant soft x-ray absorption has been extensively utilized in the study of $ReNiO_3$ perovskites.[13,55,56] The small thickness

($\sim$6 nm) of these films compares well with the probing depth ($\sim$12 nm) of the TEY mode and allows us to explore the electronic structure of the entire sample. Figure 3 shows the measured absorption for the whole range of strain values. As seen, the strong white lines at 855 and 872 eV correspond to the L_3 and L_2 edge transition from the $d^7 : t_{2g}^6 e_g^1$ ground state to the $\underline{c}t_{2g}^6 e_g^2$ ($\underline{c}$ denotes a core hole) excited state. Another lower energy peak, $\sim$853 eV, which corresponds to the same electronic transition when strong electron localization is present, becomes prominent for the highly tensile strained samples. This systematic change in the multiplet and/or L_3 relative position and intensity holds valuable information about the hybridization of the d^7 and $d^8\underline{L}$ states. The quantitative value of the observed splitting, which is simulated by tuning the charge transfer energy (Δ) is plotted in Fig. 4(b).[53] In order to obtain the peak splitting the data was fitted with two Voight functions. A direct inspection of the plot clearly shows that this splitting begins decreasing as the films are compressed in the *a-b* plane, suggesting that a change in the degree of covalency between Ni and O is likely a cause of the observed transport properties. To confirm this, *ab initio* cluster calculations were carried out using the charge transfer energy Δ as a a control parameter [see Fig. 4(b) (right side)]. The results of the calculation directly suggest that changing Δ reproduces the observed splitting well, with a value as large as $\sim$2.5 eV for the tensile strained samples and being reduced down to the very small value of $\sim$0.65 eV in the case of the all-metallic film on YAO corresponding to an enhanced degree of covalency by almost four times (spectra can be seen in Ref. 53).

The large reduction in Δ (approximately 1/4 of the saturated value for ENO on YAO) strongly implies that hybridization is strongly increased between Ni *d* and O *p* orbitals. In addition, the value of $d\ln\rho/d(\frac{1}{T})$ [Fig. 3(b)] at room temperature is approximately equal to the activation gap, showing the activation energy is steadily increased as compressive strain is reduced and nearly quenched for the tensile strained samples. The reduction of Δ and the activation gap under compressive strain can be rationalized in terms of changes in the Ni-O-Ni bond; as the lattice is compressed in plane an increase in the overlap of the O $p_{x,y}$ and Ni $d_{x^2-y^2}$ orbitals occurs. Furthermore, the increasing covalence is strongly resemblant of the effect of *A*-site cation exchange (Fig. 1).[27] On the other hand, for the tensile strained samples, the bond overlap would decrease, leading to a reduction in Ni-O hybridization, except for the fact that the splitting and transport appear to remain *unchanged* with increasing tensile strain. This observation indicates that as the strain is changed from compressive to tensile the major $d^8\underline{L}$ contribution to the ground state becomes effectively decoupled from the ionic d^7 state. It is interesting to note that these results are also compatible with the recent density-functional theory plus dynamical mean-field theory nickelate calculations, based on a site-selective Mott state, where the insulating gap is determined by the singlet formation energy between an O *p* hole and Ni *d* electron;[34] the theory also suggests the decoupling of the d^7 and the $d^8\underline{L}$ states leading to an insulating ground state. Further corroborating our results, Wang *et al.* recently suggested that the insulating regime is largely controlled by the *d*-band occupancy, and not by the

intra-electronic repulsion, which is strongly dependent on the charge transfer from oxygen ions.[57]

To summarize, epitaxial ultrathin films of ENO grown on a variety of substrates spanning both compressive and tensile strain were investigated with XRD, electric dc transport, resonant XAS, and first-principle cluster calculations. The sample's electronic properties were found to be highly tunable by strain, shifting the Mott transition tantalizingly close to room temperature and only affecting magnetic ordering transition T_N to a small extent. The absence of hysteresis indicates that the transitions remain second order, showing a key difference between epitaxial strain and A-site doping, implying that compressive strain effectively mimics external isotropic pressure. A combination of XAS and *ab initio* cluster calculations has determined that compressive strain enhances the covalence of the Ni d and O p orbitals, eventually leading to an entirely metallic ground state not accessible in the bulk. These results showcase ENO's tunability, as the MIT can be tuned from the impractically high bulk value of 480 K to near room temperature or to being entirely quenched without the complication of chemical doping.

*dmeyers@uark.edu

[1] M. Imada, A. Fujimori, and Y. Tokura, Rev. Mod. Phys. **70**, 1039 (1998).

[2] J. Chakhalian, J. W. Freeland, H.-U. Habermeier, G. Cristiani, G. Khaliullin, M. van Veenendaal, and B. Keimer, Science **318**, 1114 (2007).

[3] J. Chakhalian, J. W. Freeland, G. Sprajer, J. Strempfer, G. Khaliullin, J. C. Cezar, T. Charlton, R. Dalgliesh, C. Bernhard, G. Cristiani, H.-U. Habermeier, and B. Keimer, Nat. Phys. **2**, 244 (2006).

[4] Y. Tokura, Rep. Prog. Phys. **69**, 797 (2006).

[5] M. McCormack, S. Jin, T. H. Tiefel, R. M. Fleming, and J. M. Phillips, Appl. Phys. Lett. **64**, 22 (1994).

[6] J. Wang, J. B. Neaton, H. Zheng, V. Nagarajan, S. B. Ogale, B. Liu, D. Viehland, V. Vaithyanathan, D. G. Schlom, U. V. Waghmare, N. A. Spaldin, K. M. Rabe, M. Wuttig, and R. Ramesh, Science **299**, 1719 (2003).

[7] V. Laukhin, J. Fontcuberta, J. L. Garcia-Munoz, and X. Obradors, Phys. Rev. B **56**, R10009 (1997).

[8] H. Kuwahara, Y. Tomioka, A. Asamitsu, Y. Moritomo, and Y. Tokura, Science **270**, 961 (1995).

[9] Jian Liu, M. Kareev, D. Meyers, B. Gray, P. Ryan, J. W. Freeland, and J. Chakhalian, Phys. Rev. Lett. **109**, 107402 (2012).

[10] K. Ghosh, S. B. Ogale, R. Ramesh, R. L. Greene, T. Venkatesan, K. M. Gapchup, R. Bathe, and S. I. Patil, Phys. Rev. B **59**, 533 (1999).

[11] C. H. Ahn, J.-M. Triscone, and J. Mannhart, Nature (London) **424**, 1015 (2003).

[12] A. R. Kaul, O. Yu Gorbenko, and A. A. Kamenev, Russ. Chem. Rev. **73**, 861 (2004).

[13] Jian Liu, M. Kareev, B. Gray, J. W. Kim, P. Ryan, B. Dabrowski, J. W. Freeland, and J. Chakhalian, Appl. Phys. Lett. **96**, 233110 (2010).

[14] A. Tiwari, C. Jin, and J. Narayan, Appl. Phys. Lett. **80**, 21 (2002).

[15] Z. Chen, X. Zou, W. Ren, L. You, C. Huang, Y. Yang, P. Yang, J. Wang, T. Sritharan, L. Bellaiche, and L. Chen, Phys. Rev. B **86**, 235125 (2012).

[16] S. El Helali, K. Daoudi, A. Fouzri, M. Oumezzine, M. Oueslati, and T. Tsuchiya, Appl. Phys. A **108**, 379 (2012).

[17] A. Biswas, M. Rajeswari, R. C. Srivastava, T. Venkatesan, R. L. Greene, Q. Lu, A. L. de Lozanne, and A. J. Millis, Phys. Rev. B **63**, 184424 (2001).

[18] J. Zhang, H. Tanaka, T. Kanki, J.-H. Choi, and T. Kawai, Phys. Rev. B **64**, 184404 (2001).

[19] X. J. Chen, S. Soltan, H. Zhang, and H.-U. Habermeier, Phys. Rev. B **65**, 174402 (2002)

[20] A. T. Zayak, X. Huang, J. B. Neaton, and K. M. Rabe, Phys. Rev. B **74**, 094104 (2006).

[21] D. Fuchs, C. Pinta, T. Schwarz, P. Schweiss, P. Nagel, S. Schuppler, R. Schneider, M. Merz, G. Roth, and H. v. Lhneysen, Phys. Rev. B **75**, 144402 (2007).

[22] D. Fuchs, E. Arac, C. Pinta, S. Schuppler, R. Schneider, and H. v. Lhneysen, Phys. Rev. B **77**, 014434 (2008).

[23] A. D. Rata, A. Herklotz, K. Nenkov, L. Schultz, and K. Dorr, Phys. Rev. Lett. **100**, 076401 (2008).

[24] H. W. Jang, S. H. Baek, D. Ortiz, C. M. Folkman, R. R. Das, Y. H. Chu, P. Shafer, J. X. Zhang, S. Choudhury, V. Vaithyanathan, Y. B. Chen, D. A. Felker, M. D. Biegalski, M. S. Rzchowski, X. Q. Pan, D. G. Schlom, L. Q. Chen, R. Ramesh, and C. B. Eom, Phys. Rev. Lett. **101**, 107602 (2008).

[25] J. H. Lee and K. M. Rabe, Phys. Rev. Lett. **104**, 207204 (2010).

[26] J. H. Lee *et al.*, Nature (London) **466**, 954 (2010).

[27] María Luisa Medarde, J. Phys.: Condens. Matter **9**, 1679 (1997).

[28] J. B. Torrance, P. Lacorre, A. I. Nazzal, E. J. Ansaldo, and Ch. Niedermayer, Phys. Rev. B **45**, 8209 (1992).

[29] M. K. Stewart, Jian Liu, R. K. Smith, B. C. Chapler, C.-H. Yee, D. Meyers, R. E. Baumbach, M. B. Maple, K. Haule, J. Chakhalian, and D. N. Basov, J. Appl. Phys. **110**, 033514 (2011).

[30] A. Caytuero, H. Micklitz, M. M. Abd-Elmeguid, F. J. Litterst, J. A. Alonso, and E. M. Baggio-Saitovich, Phys. Rev. B **76**, 193105 (2007).

[31] J. E. Lorenzo, J. L. Hodeau, L. Paolasini, S. Lefloch, J. A. Alonso, and G. Demazeau, Phys. Rev. B **71**, 045128 (2005).

[32] V. Scagnoli, U. Staub, M. Janousch, A. M. Mulders, M. Shi, G. I. Meijer, S. Rosenkranz, S. B. Wilkins, L. Paolasini, J. Karpinski, S. M. Kazakov, and S. W. Lovesey, Phys. Rev. B **72**, 155111 (2005).

[33] Y. Bodenthin, U. Staub, C. Piamonteze, M. García-Fernández, M. J. Martínez-Lope, and J. A. Alonso, J. Phys.: Condens. Matter **23**, 036002 (2011).

[34] H. Park, A. J. Millis, and C. A. Marianetti, Phys. Rev. Lett. **109**, 156402 (2012).

[35] C. Piamonteze, H. C. N. Tolentino, A. Y. Ramos, N. E. Massa, J. A. Alonso, M. J. Martinez-Lope, and M. T. Casais, Physica B **320**, 71 (2002).

[36] J.-S. Zhou, J. B. Goodenough, and B. Dabrowski, Phys. Rev. Lett. **95**, 127204 (2005).

[37] G. Frand, O. Bohnke, P. Lacorre, and J. L. Forquet, J. Solid State Chem. **120**, 157 (1995).

[38] J. Chaloupka and G. Khaliullin, Phys. Rev. Lett. **100**, 016404 (2008).

[39] W. L. Lim, E. J. Moon, J. W. Freeland, D. J. Meyers, M. Kareev, J. Chakhalian, and S. Urazhdin, Appl. Phys. Lett. **101**, 143111 (2012).

[40] S. Asanuma, P.-H. Xiang, H. Yamada, H. Sato, I. H. Inoue, H. Akoh, A. Sawa, K. Ueno, H. Shimotani, H. Yuan, M. Kawasaki, and Y. Iwasa, Appl. Phys. Lett. **97**, 142110 (2010).

[41] R. Scherwitzl, P. Zubko, I. Gutierrez Lezama, S. Ono, A. F. Morpurgo, G. Catalan, and J.-M. Triscone, Adv. Mater. **22**, 5517 (2010).

[42] P. Lacorre, J. B. Torrance, J. Pannetier, A. I. Nazzal, P. W. Wang, and T. C. Huang, Journal Solid State Chem. **91**, 225 (1991).

[43] M. J. Martínez-Lope and J. A. Alonso, Eur. J. Solid State Inorg. Chem. **32**, 361 (1995).

[44] S. Middey, D. Meyers, M. Kareev, E. J. Moon, B. A. Gray, X. Liu, J. W. Freeland, and J. Chakhalian, Appl. Phys. Lett. **101**, 261602 (2012).

[45] D. Meyers, E. J. Moon, M. Kareev, I. C. Tung, B. A. Gray, J. Liu, M. J. Bedzyk, J. W. Freeland, and J. Chakhalian, arXiv:1112.5348.

[46] A. Venimadhav, C. Lekshmi, and M. S. Hegde, Mater. Res. Bull. **37**, 201 (2002).

[47] J.-G. Cheng, J.-S. Zhou, J. B. Goodenough, J. A. Alonso, and M. J. Martinez-Lope, Phys. Rev. B **82**, 085107 (2010).

[48] R. Lengsdorf, A. Barla, J. A. Alonso, M. J. Martinez-Lope, H. Micklitz, and M. M. Abd-Elmguid, J. Phys.: Condens. Matter **16**, 3355 (2004).

[49] I. I. Mazin, D. I. Khomskii, R. Lengsdorf, J. A. Alonso, W. G. Marshall, R. M. Ibberson, A. Podlesnyak, M. J. Martínez-Lope, and M. M. Abd-Elmeguid, Phys. Rev. Lett. **98**, 176406 (2007).

[50] J. Chakhalian, A. J. Millis, and J. Rondinelli, Nat. Mater. **11**, 92-94 (2012)

[51] J. Chakhalian, J. M. Rondinelli, Jian Liu, B. A. Gray, M. Kareev, E. J. Moon, N. Prasai, J. L. Cohn, M. Varela, I. C. Tung, M. J. Bedzyk, S. G. Altendorf, F. Strigari, B. Dabrowski, L. H. Tjeng, P. J. Ryan, and J. W. Freeland, Phys. Rev. Lett. **107**, 116805 (2011).

[52] M. A. van Veenendaal and G. A. Sawatzky, Phys. Rev. B **50**, 11326 (1994).

[53] Jian Liu, S. Okamoto, M. van Veenendaal, M. Kareev, B. Gray, P. Ryan, J. W. Freeland, and J. Chakhalian, Phys. Rev. B **83**, 161102(R) (2011).

[54] S. J. May, C. R. Smith, J.-W. Kim, E. Karapetrova, A. Bhattacharya, and P. J. Ryan, Phys. Rev. B **83**, 153411 (2011).

[55] M. Mizumaki, N. Ishimatsu, N. Kawamura, M. Azuma, Y. Shimakawa, M. Takano, and T. Uozumi, Phys. Rev. B **80**, 233104 (2009).

[56] M. Medarde, A. Fontaine, J. L. García-Muñoz, J. Rodríguez-Carvajal, M. De Santis, M. Sacchi, G. Rossi, and P. Lacorre, Phys. Rev. B **46**, 14975 (1992).

[57] X. Wang, M. J. Han, Luca de' Medici, H. Park, C. A. Marianetti, and A. J. Millis, Phys. Rev. B **86**, 195136 (2012).